

Auroral zone over the last 3000 years

Ryuhō Kataoka^{1,4,*} and Shin'ya Nakano^{2,3,4}

¹ National Institute of Polar Research, 10-3 Midori-cho, Tachikawa, Tokyo 190-8518, Japan

² The Institute of Statistical Mathematics, 10-3 Midori-cho, Tachikawa, Tokyo 190-8562, Japan

³ Center for Data Assimilation Research and Applications, Joint Support Center for Data Science Research, 10-3 Midori-cho, Tachikawa, Tokyo 190-8562, Japan

⁴ The Graduate University for Advanced Studies, SOKENDAI, Shonan Village, Hayama, Kanagawa 240-0193, Japan

Received 21 April 2021 / Accepted 28 July 2021

Abstract – We investigated the global shape of the auroral zone over the last 3000 years using paleomagnetism CALS models. A similar method of apex latitude as proposed by Oguti (1993) [J Geophys Res **98** (A7): 11649–11655; J Geomag Geoelectr **45**, 231–242] was adopted to draw the auroral zone. The Oguti method is examined using 50-year data from ground-based magnetometers located at high latitudes, using International Geomagnetic Reference Field (IGRF) models. The equatorward auroral limit during magnetic storms was also examined using more than 20 years of data from the Defense Meteorological Satellite Program (DMSP) satellites. The reconstructed auroral zone and the equatorward auroral limit were compared with the historical auroral witness records for 1200 AD and 1800 AD. We concluded that the 12th and 18th centuries were excellent periods for Japan and the United Kingdom, respectively, to observe auroras over the last 3000 years.

Keywords: Aurora, magnetic storm, paleomagnetism

1 Introduction

Matsushita (1956) briefly summarized that *Nippon Kisho-Shiryō* provided historical data for remarkable meteorological occurrences, including auroras, even from middle-latitude Japan. Among these records, a significant portion of the auroral witnesses has clustered around the year 1200 AD. As an example, curtain-like auroras (white and red lights crossing each other) appeared to the north of Kyoto, Japan (35° N, 135° E in geographic coordinates) for several nights in February 1204 AD, documented in *Meigetsuki* (Kataoka et al., 2017).

Keimatsu et al. (1968) reported that the geomagnetic dipole axis might have been inclined toward China around the 11th–12th century, based on the simultaneously observed southern boundary of auroras in Europe and China. Siscoe (1980) also discussed that solar activity must have been relatively high in the 12th century, based on the number of auroral records that peaked during this period in China and Europe.

This paper aims to examine whether the 12th century was the best age for Japan to observe auroras. This will be accomplished by drawing the shape of the auroral zone for the last 3000 years – using the latest Gauss coefficients with higher

degrees than a simple dipole. The obtained results were compared with notable historical records worldwide.

2 Auroral zones from 1960 to 2010 AD using IGRF models

To estimate the magnetic latitude in the past, dip latitude, as estimated from the inclination angle of the local magnetic field, can be used (e.g., Lockwood & Barnard, 2015; Kataoka et al., 2017), as well as dipole latitude. Potential challenges exist for both methods; that is, a local anomaly may influence the results significantly if the dip latitude is used, and the complex magnetic fields may be oversimplified if the dipole latitude is used – due to omitting higher-order Gauss coefficients.

To include higher-order terms, a method similar to that proposed by Oguti (1993a) was adopted to draw the auroral zone. Recently, Tsyganenko (2019) applied an advanced method using an external field to discuss the secular drift of the auroral zone and obtained consistent results with those from Oguti (1993a). We used International Geomagnetic Reference Field (IGRF) models (Alken et al., 2021, and references therein) to find the ionospheric footprints of the apex field intensities – 49, 173, 474, and 6178 nT – as the equivalent dipole latitudes

*Corresponding author: kataoka.ryuho@nipr.ac.jp

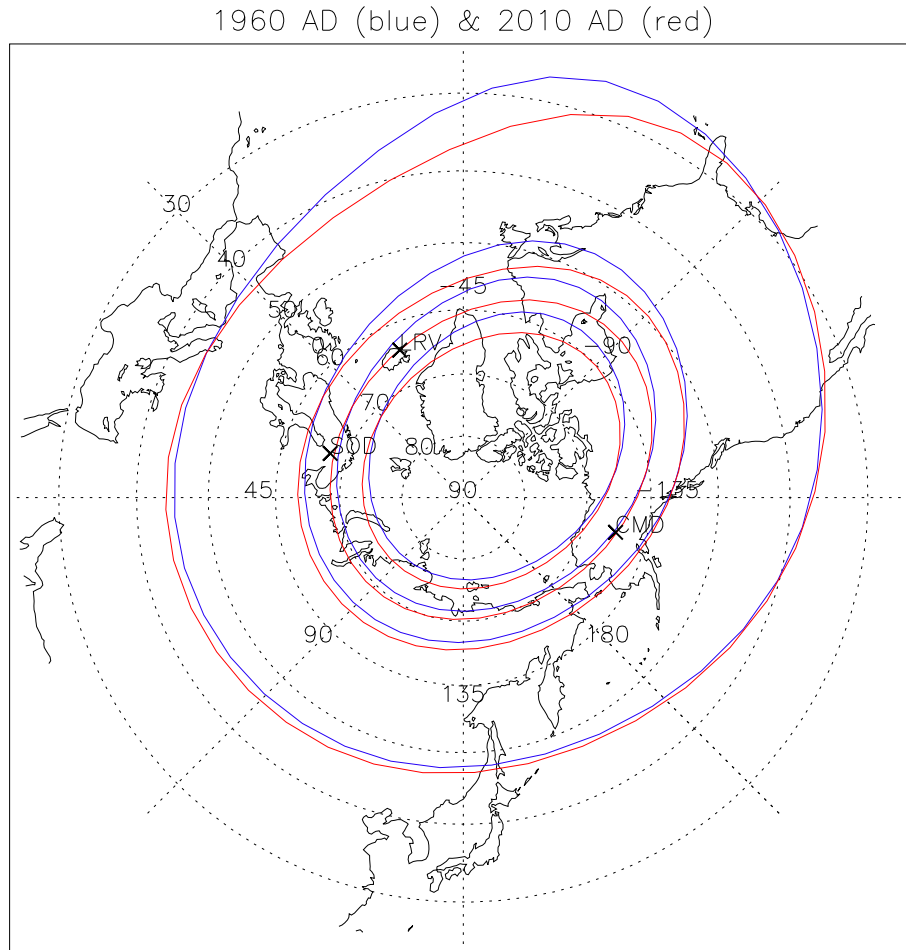


Fig. 1. Reconstructed global shape of the auroral zone in 1960 AD (blue) and 2010 AD (red). Contours are apex field intensities of 49, 173, 474, and 6178 nT, corresponding to 70, 65, 60, and 40 magnetic latitudes. Japan's longitude (135° E) is toward the bottom. The positions of LRV (Leirvogur, Iceland), SOD (Sodankylä, Finland), and CMO (College, Alaska) are marked by crosses.

of 70°, 65°, 60°, and 40°, respectively. The apex magnetic latitude can also be computed by tracing the magnetic field line at the desired point to the apex of the magnetic field line to provide the corresponding latitude of the reference dipole (e.g., [Richmond, 1995](#)).

The auroral zone can be defined by the belt between the 70° and 65° contours and the sub-auroral zone defined by the belt between 65° and 60°. The auroral oval extends over the sub-auroral zone during magnetic storms. [Keimatsu et al. \(1968\)](#) discussed that a magnetic latitude of 40° roughly corresponds to an annual average auroral isochasm of 0.1 ([Fritz, 1881](#)). A recent collection of historical auroral records shows that auroral witnesses drastically increased above the 40° magnetic latitude ([Vasquez et al., 2016](#)). Auroras appearing at 40° magnetic latitude can be viewed from an observation site at equatorward of 40° because the altitude of emission is high at above ~400 km. The magnetic storm that occurred in February 1958 is a contemporary example. The red aurora at a magnetic latitude of 40° was seen from at Niigata Prefecture at a 27.5° magnetic latitude ([Kataoka et al., 2019](#); [Kataoka & Kazama, 2019](#)).

The reconstructed auroral zone and the equatorward auroral limit of 40° for 1960 AD and 2010 AD are shown in [Figure 1](#).

The time variation of the auroral zones can be validated by the accumulated data from ground-based magnetometers, while data from the Defense Meteorological Satellite Program (DMSP) spacecraft can also validate the equatorward auroral limit.

3 Auroral zones as identified by magnetometers and DMSP satellites

We show that the apex latitude is a good indicator of the auroral zone using 50-year data from ground-based magnetometers. The Z-component helps identify the relative latitudinal position against the westward auroral electrojet. This is because Z becomes positive (downward in the Northern Hemisphere) if the magnetometer is located at the poleward side of the westward auroral electrojet and vice versa. The selected high-latitude magnetic observatories were LRV (Leirvogur Magnetic Observatory, Iceland; 64.18° N, 338.3° E in geographic coordinates), SOD (Sodankylä, Geophysical Observatory, Finland; 67.37° N, 26.63° E), and CMO (College International Geophysical Obser-

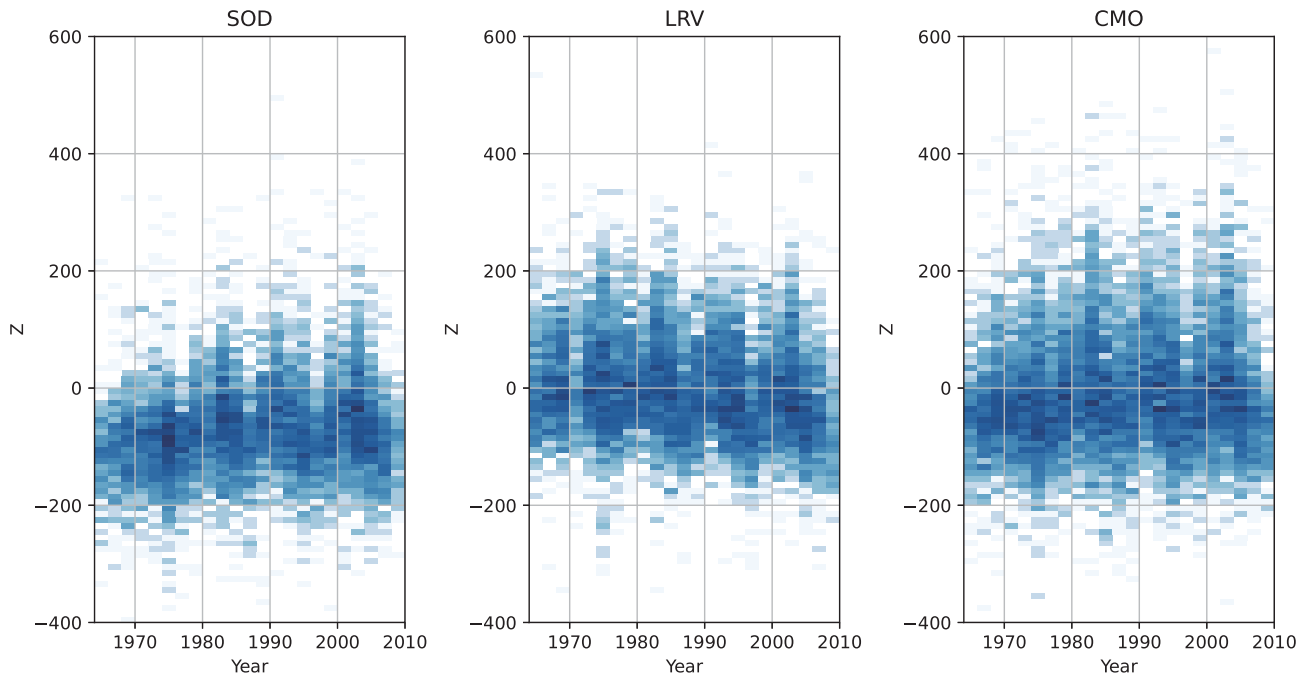


Fig. 2. Occurrence distribution of the Z component for the conditions of $-50 \text{ nT} \leq Dst < 0$ and $H < -100 \text{ nT}$. SOD: $23 \leq UT < 2$ (left), LRV: $2 \leq UT < 5$ (middle), and CMO: $13 \leq UT < 16$ (right).

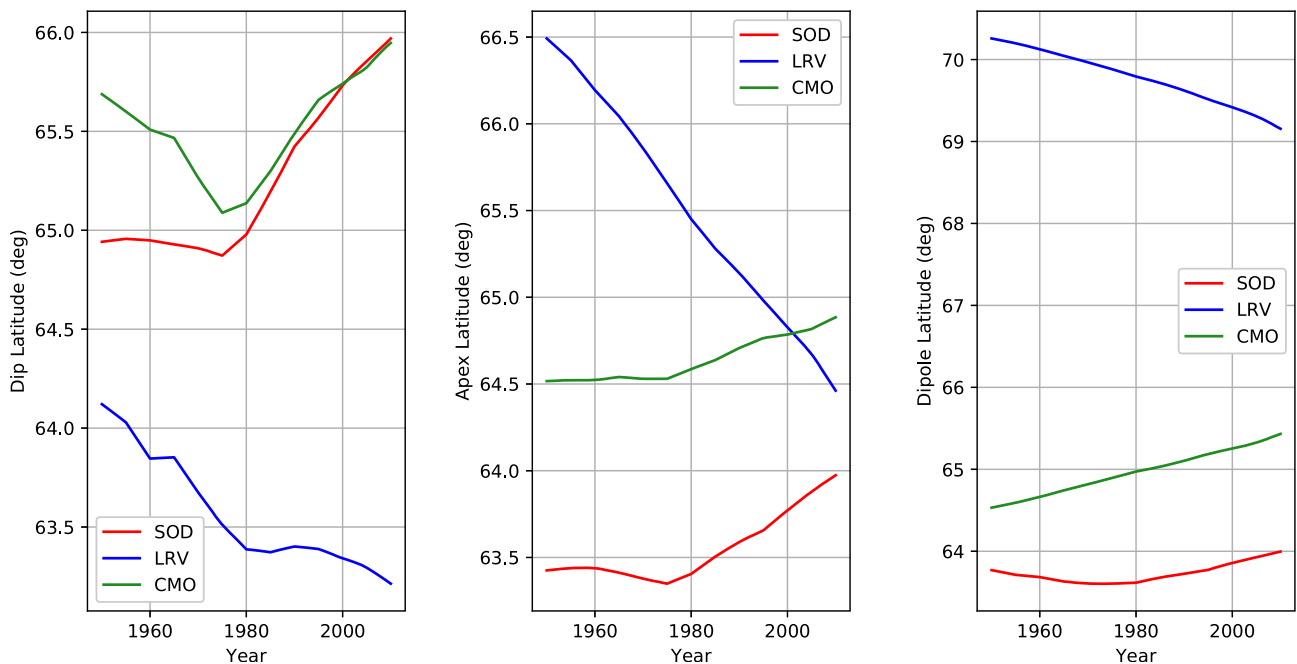


Fig. 3. Dip latitude (left), apex latitude (middle), and dipole latitude (right) of ground-based magnetometers at SOD, LRV, CMO.

vatory, Alaska; 64.87° N , 212.14° E). Since both eastward and westward electrojets exist (e.g., Kamide & Kokubun, 1996, and references therein), we limited our analysis to the post-midnight sector of 2–5 magnetic local time sector (see the UT range for each station in the caption of Figure 2), where westward electrojets are dominant (Allen & Kroehl, 1975).

Figure 2 shows the distribution of the hourly value of the Z-component observed at LRV, SOD, and CMO for 50 years since 1960 AD. Moderate geomagnetic activity of $Dst \geq -50 \text{ nT}$ and $H \leq -100 \text{ nT}$ was selected. Positive and negative trends can be found in Z for SOD and LRV, respectively.

Table 1. Results of the metropolis method for Equation (1).

	a0	b0	b1
LRV	-1.9225 ± 0.0283	-30.8371 ± 0.6122	-0.6212 ± 0.0335
SOD	-1.8453 ± 0.0305	-56.6877 ± 0.8133	0.5227 ± 0.0432
CMO	-2.5639 ± 0.0359	-21.8977 ± 0.5592	0.1713 ± 0.0295

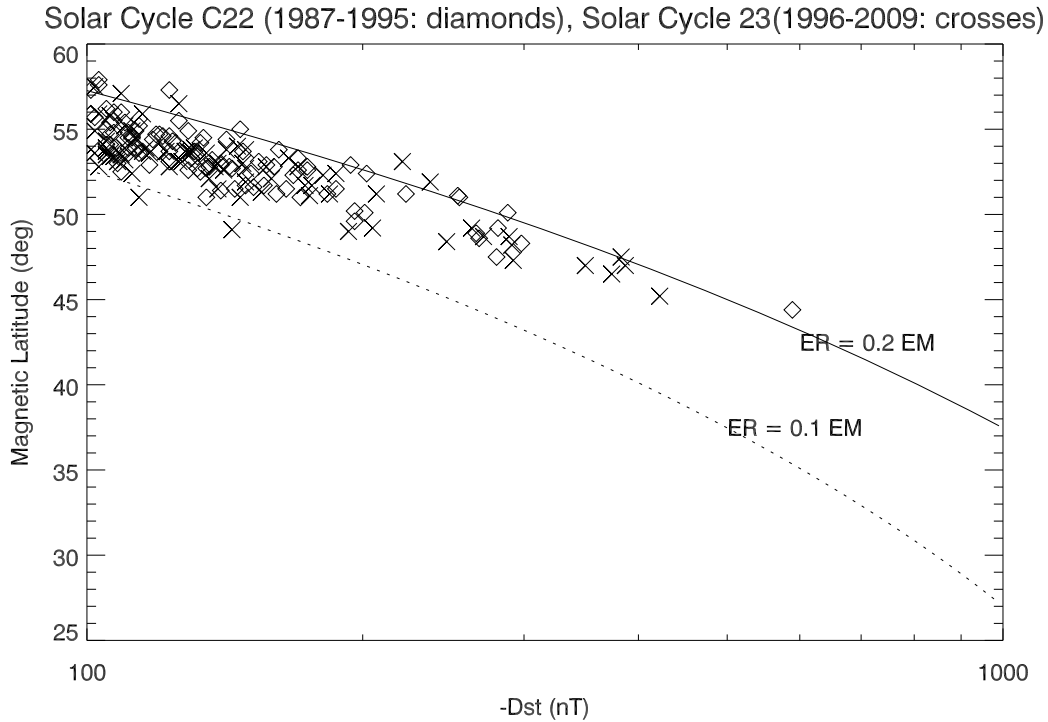


Fig. 4. Minimum magnetic latitude of the auroral equatorial boundary against the peak intensity of magnetic storms. Diamonds and crosses show the scatter plots for solar cycle 22 (1987–1995) and solar cycle 23 (1996–2009), respectively. Dotted and solid lines show the 10% and 20% efficiency to transform ER from EM, respectively.

The trends identified in Figure 2 can be interpreted as the long-term variation of the apex magnetic latitude of the magnetometers, as shown in Figure 3. The auroral zone was located at a constant apex magnetic latitude of $\sim 65^\circ$ for 50 years, as confirmed by Figure 1. Note that the other dip latitude or dipole latitude method, as shown in Figure 3, fails to explain Figure 2. The dipole latitude of LRV is high at $> 69^\circ$, indicating that the dipole latitude does not explain Figure 2, although LRV has been under the auroral oval for decades.

The auroral oval extends equatorward during magnetic storms (e.g., Yokoyama et al., 1998). The equation below is used to distinguish between the long-term trend and the *Dst* effect on the *Z*-component data for the disturbing activity of $H < -100$ nT:

$$Z = a_0[Dst - b_0 - b_1(\text{year} - 2000)]. \quad (1)$$

The parameters are estimated as the Bayesian posterior distribution under a flat prior, obtained using the Metropolis method (Robert & Casella, 2004). The results are shown in Table 1. The positive and negative values of b_1 for SOD and LRV are consistent with the positive and negative trends of their apex magnetic latitude. In contrast, a nearly zero value of CMO

implies that CMO continued to stay under the auroral electrojet for 50 years. The expected negative correlation between *Z* and the *Dst* index appeared as negative a_0 values for all stations.

In this study, we omitted the possible effect of the variation in the magnetic moment on the shape of the auroral zone because a recent global simulation study suggested that such an effect is complex; only an $\sim 10\%$ change in the magnetic moment for the last 100 years may not be enough to observe the possible effect (Ebihara & Tanaka, 2020).

A correction of the magnetic moment may be required to compare the possible amplitudes of magnetic storms in different ages. It is true especially when they are indirectly estimated from the equatorial edge of the extended auroral oval, as Kataoka & Iwahashi (2017) discussed, following the original work by Yokoyama et al. (1998). For example, there is a 0.6% difference in the magnetic moment between solar cycles 22 and 23. It is expected that such a difference can systematically change the relationship between the ring current energy ER (converted from *Dst* minimum using $ER = 4 \times 10^{13} (-Dst)$ [J]), and magnetic energy EM (converted from the magnetic latitude of the auroral equatorial boundary – using $EM = 8 \times 10^{17} \cos^6$

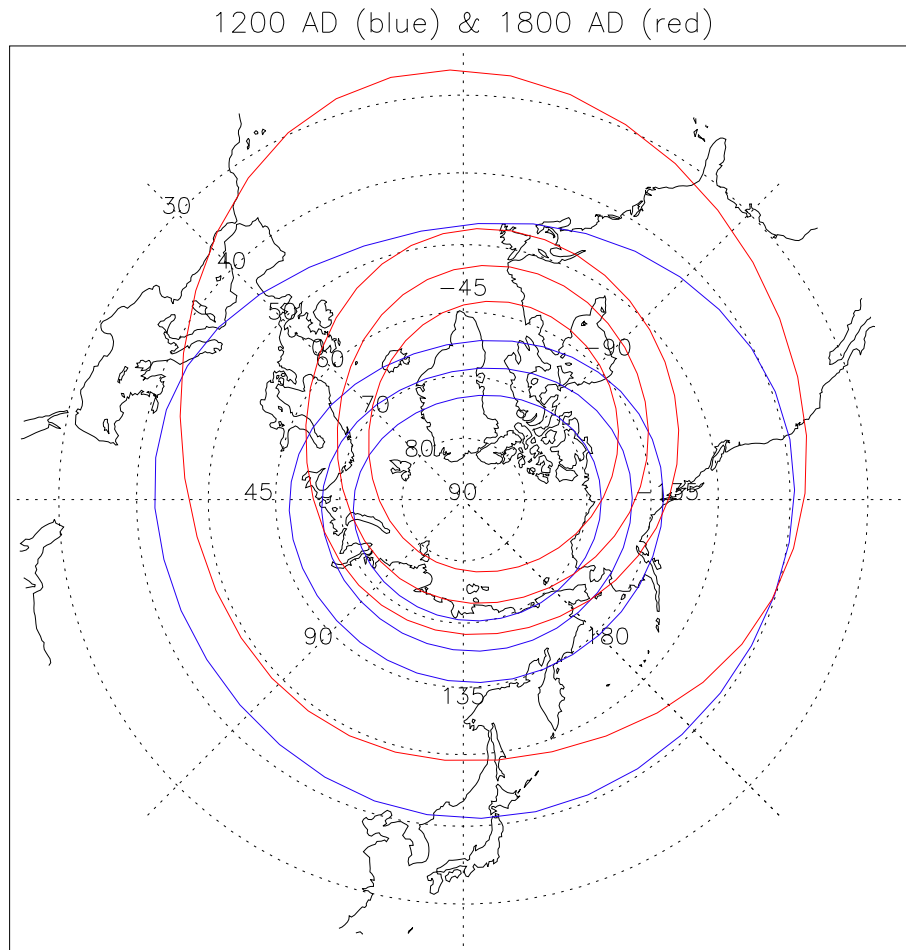


Fig. 5. Estimated global shape of the auroral zone in 1200 AD (blue) and 1800 AD (red). Contours are apex field intensities of 49, 173, 474, and 6178 nT, corresponding to 70, 65, 60, and 40 magnetic latitudes. Japan's longitude (135 E) is toward the bottom.

(magnetic latitude) [J]). However, the effect of the change in the magnetic moment would be too small to be observationally differentiated.

The auroral boundary index (ABI) is an estimate of the equatorward boundary of precipitating auroral electrons, as determined by the SSJ/4 (F06 through F15) and SSJ/5 (F16 and beyond) instruments on the DMSP spacecraft (Gussenhoven et al., 1981, 1983, Hardy et al., 2008). We selected intense magnetic storm events with Dst minimum < -100 nT to determine the minimum magnetic latitude of the ABI during the ± 6 -hour time interval across the Dst minimum. The corrected magnetic latitude was used in the ABI, which provided essentially similar values to the apex magnetic latitudes. Figure 4 shows the scatter plots using the Dst index and ABI. If the data points follow the dotted and solid lines, it can be interpreted that 10% and 20% of EM became ER, respectively. The data points scatter between 10% and 20% efficiency lines, and it is difficult to find the possible systematic difference due to the magnetic moment between solar cycles 22 and 23. We also found that stronger storms followed a 20% line rather than a 10% line. Understanding the possible effect of variable magnetic moments on the extent of the auroral oval during extreme magnetic storms is an interesting challenge for future ring current simulations.

4 Auroral zone from 1000 BC to 1900 AD using CALS models

Although the use of the apex method was validated for the last 50 years when the change of magnetic moment was relatively small, it is impossible to similarly validate the use of the same method to the ancient data where the change of magnetic moment was relatively large. To evaluate the possible uncertainty, however, the possible shift of auroral zone due to the change of magnetic moment can be speculated as follows: The CALS models (Korte & Constable, 2011) indicate that the magnetic moment could be $\sim 15\%$ and $\sim 30\%$ larger than the present value for the last 1500 years and 1000 BC to 500 AD, respectively. Considering the simulation results by Ebihara & Tanaka (2020), the magnetic latitude of the estimated auroral zone can be $\sim 1^\circ$ and $\sim 2^\circ$ higher for the last 1500 years and 1000 BC to 500 AD, respectively. Hereafter we omit such a possible contribution of the magnetic moment and assume that the same apex method for the last 50 years can also be applied to the ancient data, as long as the magnetic latitude changes are significantly larger than 1 or 2 degrees.

To obtain the auroral zone in the last 3000 years, we used the Gauss coefficients of CALS3k.4b (Korte & Constable, 2011).

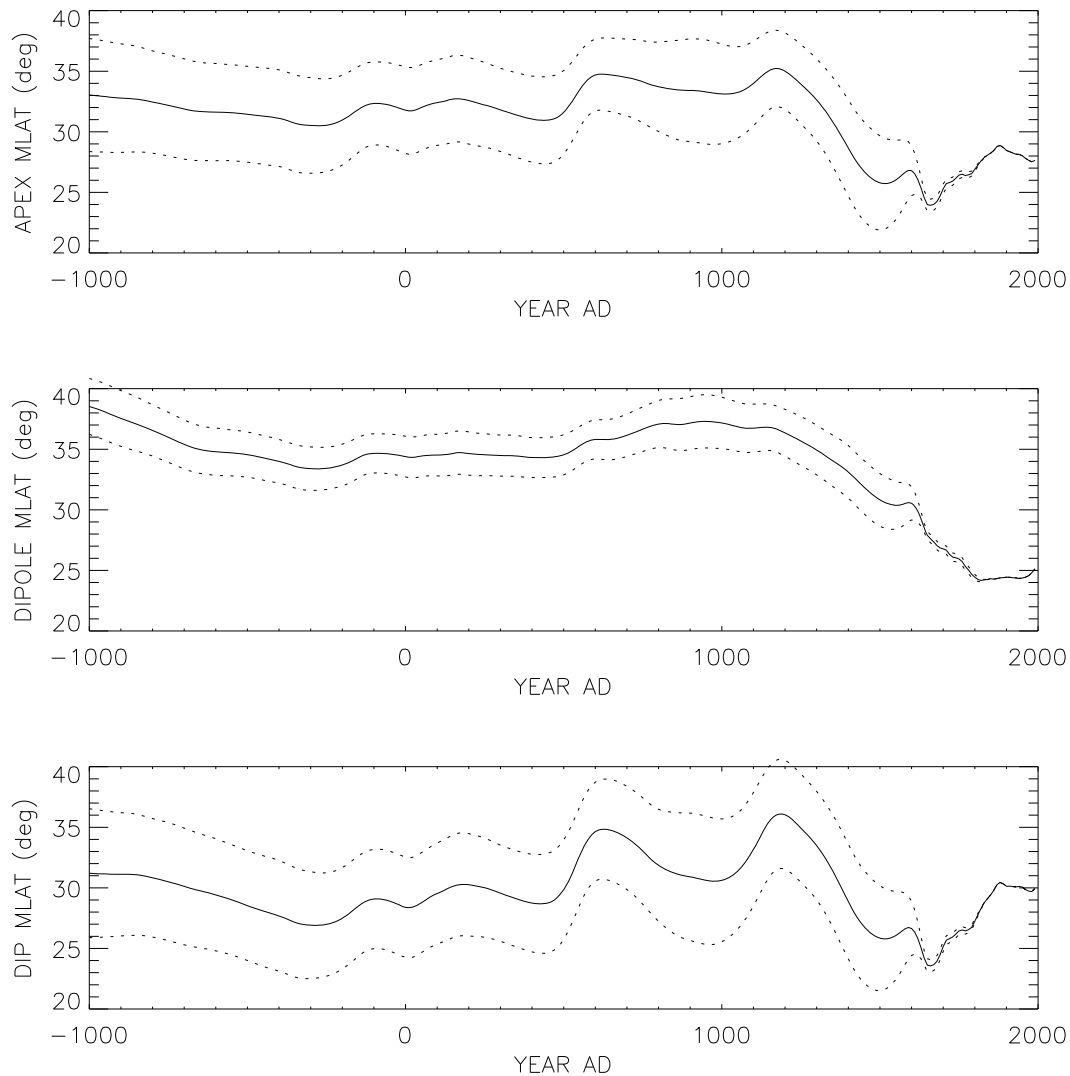


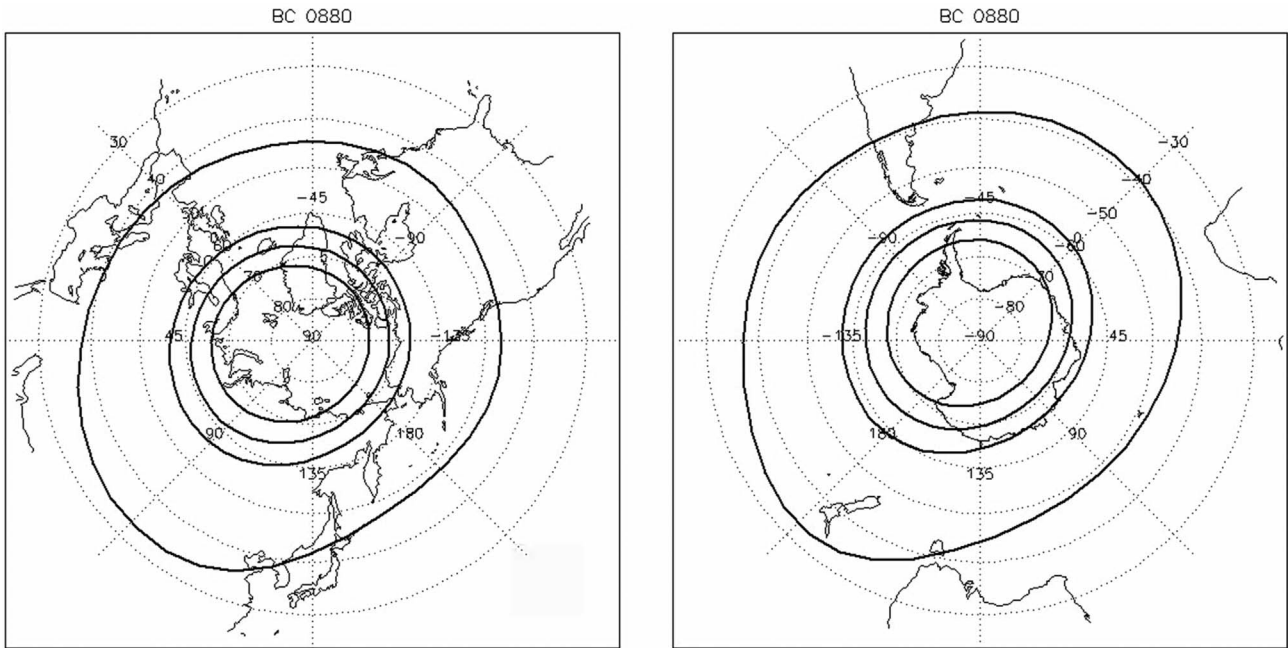
Fig. 6. Magnetic latitudes of Kyoto (35° N, 135° E) for the last 3000 years. From top to bottom, the apex latitude, dipole latitude, and dip latitude are shown. The possible errors (dotted lines) increase before 1600 AD.

Figure 5 illustrates the auroral zone in 1200 AD and 1800 AD in the Northern Hemisphere, when Japan and the UK were closest to the auroral zone, respectively. Movie 1 shows the auroral zones in the Northern and Southern Hemispheres. The CALS10k.2 model was used to calculate the auroral zone over 10,000 years (Movie 2) and to observe the possible variation of the auroral zone over a longer period. Note that the magnetic latitude changes are larger than 5 degrees, as shown in Figure 5, Movies 1, and 2. In a different manner, Korte & Stolze (2016) combined solar activity reconstruction with the CALS10k model to examine the historical auroral activity in the middle latitudes over the Holocene.

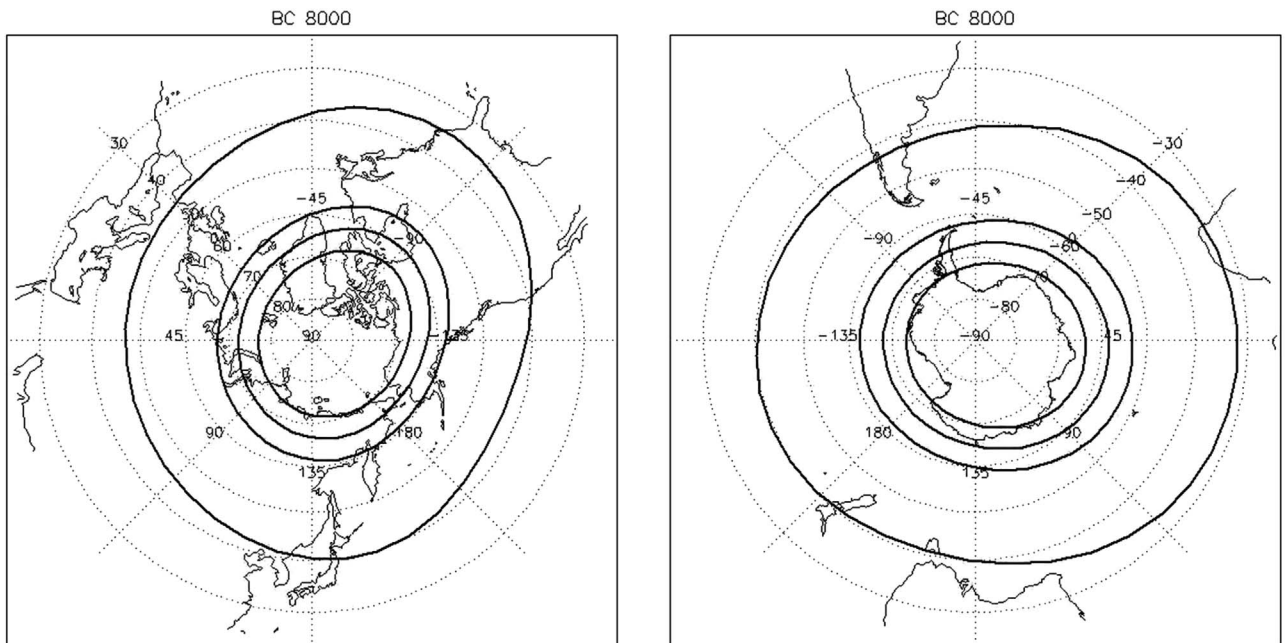
Figure 6 shows the magnetic latitude of Kyoto's position (35° N, 135° E) over the last 3000 years, using the CALS3k.4b model. The uncertainties were calculated as the standard deviation of 100 samples drawn according to the uncertainties of the CALS3k.4b model. Note again that the magnetic latitude changes are larger than 5 degrees. Kataoka et al. (2017) used the dip latitude to conclude that 1100–1200 AD was an excellent period for Japan to observe auroras. Interestingly, another

peak was found in 600 AD, when the very first evidence of auroras was recorded in Japan in December 620 AD (Kataoka et al., 2020). Hirooka (1971) observed high inclination angles of $55\text{--}60^{\circ}$ in Southeast Japan in 600–700 AD and ~ 1200 AD and a small inclination angle of $\sim 35^{\circ}$ in the 16th century. It is also notable that the continuous Chinese records of auroral witnesses from 900 AD to 1200 AD show that auroral activity was relatively weak in 1010–1050 AD when the solar activity was in one of the grand minimum conditions, called Oort Minimum (Kataoka et al., 2017).

Brekke & Egeland (1980) noted that “*The Poetic Edda*,” which does not include evidence of auroras, was most likely assembled in southern Norway between 1000 and 1100 AD – when the auroral zone covered northern Norway in the same manner as the present time. Considering the weak solar activity in the Oort Minimum, the lack of auroras in “*The Poetic Edda*” is consistent with the reconstructed auroral zone in Figure 5. “*The King's Mirror*,” in contrast, stated that the aurora was observed in Greenland in 1200 AD (Brekke & Egeland, 1980). This is also consistent with the fact that Greenland



Movie 1. Reconstructed auroral zone over the last 3000 years. CALS3k.4b was used before 1900 AD, while the IGRF models were used after 1900 AD.



Movie 2. Reconstructed auroral zone over the last 10,000 years. CALS10k.2 was used.

was located under the auroral zone in 1200 AD, as shown in Figure 5. It is also worth noting from Movie 1 that the auroral zone rapidly moved $\sim 3^\circ$ to the north in Norway from 1000 AD to 1150 AD, while the auroral zone did not change in Greenland. Such a difference may solve the discrepancy of the relative disappearance of aurora in Norway in “*The King’s Mirror*,” as Oguti & Egeland (1995) discussed.

The reconstructed auroral zone in this study is also consistent with the increased number of auroral witnesses across

Europe in the 18th century. Oguti (1993b) discussed that the northern part of the UK was located at or close to the auroral zone in the 18th century. Lockwood & Barnard (2015) recently discussed the best age for aurora observation in the UK in detail, just after the end of another grand minimum, called the Maunder Minimum.

As shown in Figures 7 and 8, the deformed auroral isochoasm by Fritz (1881) is consistent with the reconstructed auroral zone. The minimum latitudes of the auroral zone during

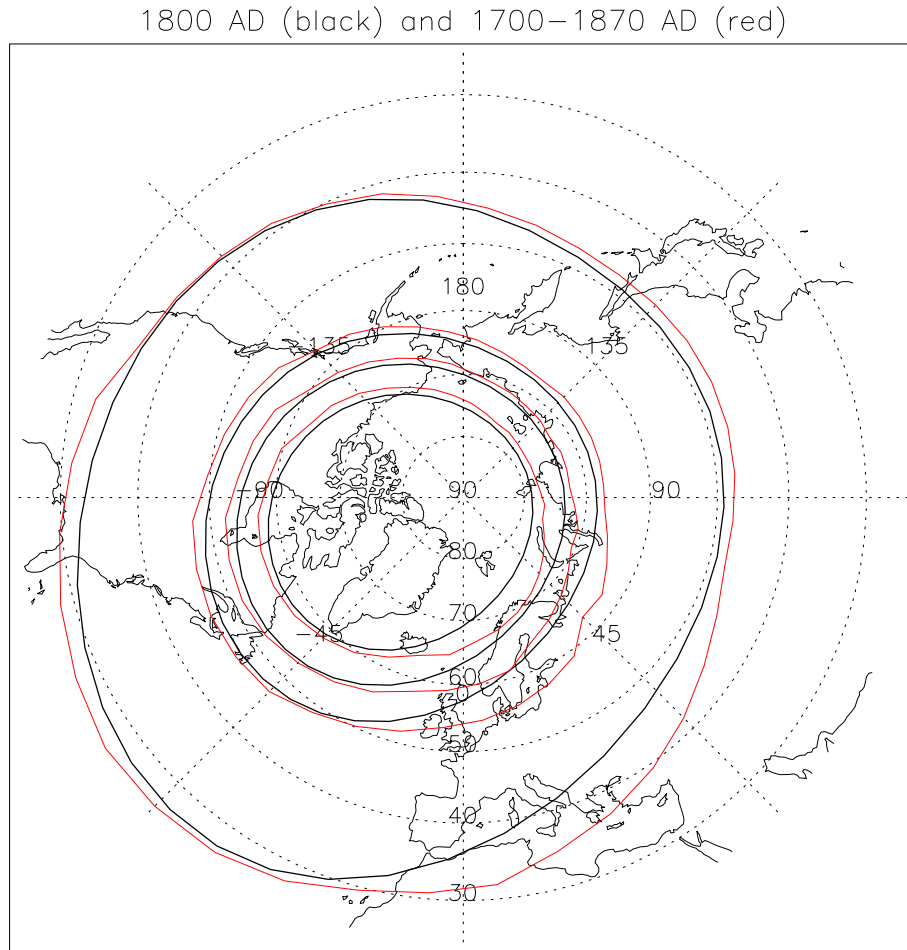


Fig. 7. Reconstructed auroral zone in 1800 AD (black) and possible deformation by a 170-year integration for the time interval between 1700 AD and 1870 AD (red).

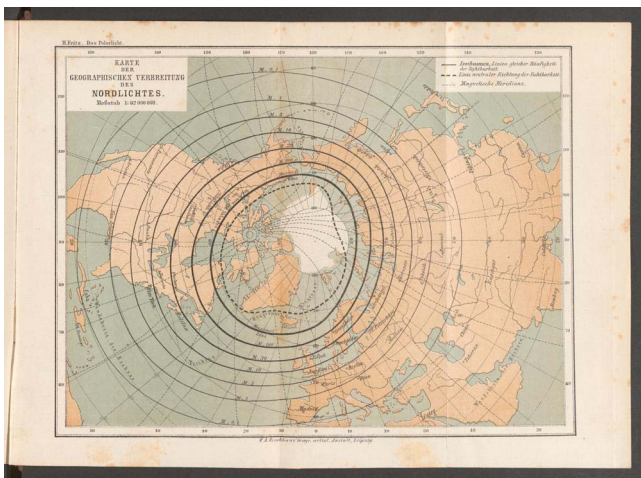


Fig. 8. Auroral isochasm by Fritz (1881). The compiled documents were from 1700 to 1872 AD.

the 170-year interval from 1700 to 1870 AD are shown in red. The deformation of the auroral zone toward the UK, as shown in Figure 8, can be understood as the motion of the auroral zone

during the 172-year time interval from 1700 to 1872 AD, as was also discussed in detail by Oguti (1993c). Comparing Figures 7 and 8, we found that the 0.1–1.0-per-year contour roughly corresponds to a 40° apex latitude, while the 10–30-per-year contour roughly corresponds to a 60° apex latitude, beneficial for comparison with other historical records.

5 Conclusions

We updated the works of Oguti (1993a, 1993b, 1993c) by defining the auroral zone with an additional 40° contour as an equatorward auroral limit to interpret historical auroral witness data – using the paleomagnetism CALS models. The IGRF models and the space-age data of the last 50 years imply that the auroral zone defined by the apex latitude is more accurate than the dipole latitude or dip latitude. We concluded that the 12th and 18th centuries were excellent periods of auroral observations for Japan and the UK, respectively, over the last 3000 years.

Acknowledgements. The authors thank the fruitful discussions with Shigeru Fujita, Kiyoka Murase, Kazuaki Yamamoto, and Hidetoshi Shibuya. The Air Force Research Laboratory ABI

was provided by the United States Air Force Research Laboratory, Kirtland Air Force Base, New Mexico. ABI data are available in yearly ASCII files below, at the CEDAR Madrigal Archive at <http://cedar.openmadrigal.org>. We acknowledge the use of CALS models and IGRF models. The geomagnetic field data used in this paper were obtained in College, Sodankylä, Leirvogur observatories, and provided by the WDC for Geomagnetism, Kyoto (<http://wdc.kugi.kyoto-u.ac.jp/wdc/Sec3.html>). The Dst index is provided from Kyoto University (World Data Center for Geomagnetism Kyoto, M. Nose, T. Iyemori, M. Sugiura, T. Kamei (2015), Geomagnetic Dst index, <https://doi.org/10.17593/14515-74000>). This work was supported by the Project of Build an International Collaborative Research for Pre-modern Japanese Texts. The editor thanks Natalia-Silvia Asimopolos and an anonymous reviewer for their assistance in evaluating this paper.

References

- Alken P, Thébaud E, Beggan CD, Amit H, Aubert J, et al. 2021. International geomagnetic reference field: the thirteenth generation. *Earth Planets Space* **73**: 49. <https://doi.org/10.1186/s40623-020-01288-x>.
- Allen JH, Kroehl HW. 1975. Spatial and temporal distributions of magnetic effects of auroral electrojets as derived from AE indices. *J Geophys Res* **80(25)**: 3667–3677.
- Brekke A, Egeland A. 1980. Ancient Norwegian literature in relation to the auroral oval. In: *Exploration of the Polar Upper Atmosphere*. Deehr CS, Holtet JA, (Eds.), Reidel, Dordrecht, pp. 431–442.
- Ebihara Y, Tanaka T. 2020. How do auroral substorms depend on Earth's dipole magnetic moment? *J Geophys Res Space Phys* **126**: e2020JA028009. <https://doi.org/10.1029/e2020JA028009>.
- Fritz H. 1881. *Das Polarlicht*. F.A. Brockhaus, Leipzig. <https://doi.org/10.3931/e-rara-2131>.
- Gussenhoven MS, Hardy DA, Burke WJ. 1981. DMSP/F2 electron observations of equatorward auroral boundaries and their relationship to magnetospheric electric fields. *J Geophys Res* **86**: 768–778.
- Gussenhoven MS, Hardy DA, Heinemann N. 1983. Systematics of the equatorward diffuse auroral boundary. *J Geophys Res* **88**: 5692–5708.
- Hardy DA, Holeman EG, Burke WJ, Gentile LC, Bounar KH. 2008. Probability distributions of electron precipitation at high magnetic latitudes. *J Geophys Res* **113**: A6. <https://doi.org/10.1029/2007JA012746>.
- Hirooka K. 1971. Archaeomagnetic study for the past 2000 years in southwest Japan, Memoirs of the Faculty of Science, Kyoto University. *Series of Geol Mineral* **XXXVIII**, 2: 167–207.
- Kamide Y, Kokubun S. 1996. Two-component auroral electrojet: Importance for substorm studies. *J Geophys Res* **101(A6)**: 13027–13046.
- Kataoka R, Iwahashi K. 2017. Inclined zenith aurora over Kyoto on 17 September 1770: Graphical evidence of extreme magnetic storm. *Space Weather* **15**: 1314–1320. <https://doi.org/10.1002/2017SW001690>.
- Kataoka R, Isobe H, Hayakawa H, Tamazawa H, Kawamura AD, Miyahara H, Iwasaki K, Yamamoto K, Takei M, Terashima T, Suzuki H, Fujiwara Y, Nakamura T. 2017. Historical space weather monitoring of prolonged aurora activities in Japan and in China. *Space Weather* **15(2)**: 392–402. <https://doi.org/10.1002/2016SW001493>.
- Kataoka R, Uchino S, Fujiwara Y, Fujita S, Yamamoto K. 2019. Fan-shaped aurora as seen from Japan during a great magnetic storm on 11 February 1958. *J Space Weather Space Clim* **9**: A16. <https://doi.org/10.1051/swsc/2019013>.
- Kataoka R, Kazama S. 2019. A watercolor painting of northern lights seen above Japan on 11 February 1958. *J Space Weather Space Clim* **9**: A28. <https://doi.org/10.1051/swsc/2019027>.
- Kataoka R, Yamamoto K, Fujiwara Y, Shiomi K, Kokubun N. 2020. Pheasant tail: Consideration of the shape of the red sign in the Nihon-Shoki. *Sokendai Rev. Cultural Social Stud* **16**: 17–28.
- Keimatsu M, Fukushima N, Nagata T. 1968. Archaeo-aurora and geomagnetic secular variation in historic time. *J Geomag Geoelectr* **20(1)**: 45–50.
- Korte M, Constable C. 2011. Improving geomagnetic field reconstructions for 0–3 ka. **188**, 3-4, 247–259. <https://doi.org/10.1016/j.pepi.2011.06.017>.
- Korte M, Stolze S. 2016. Variations in mid-latitude auroral activity during the Holocene. *Archaeometry* **58(1)**: 159–176.
- Lockwood M, Barnard L. 2015. An arch in the UK. *Astron Geophys* **56**: 4.254.30. <https://doi.org/10.1093/astrogeo/atv132>.
- Matsushita S. 1956. Ancient aurorae seen in Japan. *J Geophys Res* **61**: 297–302.
- Oguti T. 1993a. Prediction of the location and form of the auroral zone: Wandering of the auroral zone out of high latitudes. *J Geophys Res* **98(A7)**: 11649–11655.
- Oguti T. 1993b. The auroral zone in historic times – The northern UK was in the auroral zone 300 years ago-. *J Geomag Geoelectr* **45**: 231–242.
- Oguti T. 1993c. A note on the auroral frequency charts by Fritz and Vestine. *J Geomag Geoelectr* **45**: 449–454.
- Oguti T, Egeland A. 1995. Auroral occurrences in Norwegian archives. *J Geomag Geoelectr* **47**: 353–359.
- Yokoyama N, Kamide Y, Miyaoka H. 1998. The size of the auroral belt during magnetic storms. *Ann Geophys* **16**: 566–573. <https://doi.org/10.1007/s00585-998-0566-z>.
- Richmond AD. 1995. Ionospheric electrodynamics using magnetic apex coordinates. *J Geomag Geoelectr* **47**: 191–212.
- Robert CP, Casella G. 2004. *Monte Carlo statistical methods*, 2nd edn. Springer Science+Business Media Inc., New York.
- Siscoe GL. 1980. Evidence in the auroral record for secular solar variability. *Rev Geophys Space Phys* **18(3)**: 647–658.
- Tsyganenko NA. 2019. Secular drift of the auroral ovals: How fast do they actually move? *Geophys Res Lett* **46**: 3017–3023. <https://doi.org/10.1029/2019GL082159>.
- Vasquez M, Vaquero JM, Gallego MC, Roca Cortes T, Palle PL. 2016. Long-term trends and Gleissberg cycles in aurora borealis records (1600–2015). *Solar Phys* **291**: 613–642. <https://doi.org/10.1007/s11207-016-0849-6>.

Cite this article as: Kataoka R & Nakano S 2021. Auroral zone over the last 3000 years. *J. Space Weather Space Clim.* **11**, 46. <https://doi.org/10.1051/swsc/2021030>.